Available online www.ejaet.com

European Journal of Advances in Engineering and Technology, 2020, 7(5):33-41

Research Article ISSN: 2394 - 658X

Colligative Properties of Surfactant-coated Nanoparticle Hydrocarbon-based Magnetic Fluids: The Influence of Magnetic Field

Gunars Kronkalns* and Mikhail Maiorov

Institute of Physics, University of Latvia
**Corresponding Author: kron@sal.lv*

ABSTRACT

In the thermodynamic processes of heat and mass transfer very important are the colligative properties of the working medium. In this connection the intensive use (application) of magnetic fluids in different industries and in medicine makes relevant the investigation of these properties for such media. The purpose of this study is to investigate the colligative properties of dispersions of single-domain magnetic nanoparticles coated with surfactant molecules and suspended in a hydrocarbon carrier fluid, and to investigate also the possible influence of the magnetic field on these properties. In this work, the samples of such hydrocarbon-based magnetic fluids with surfactant-coated ferrite nanoparticles (SNHMF) where prepared on the base of hydrocarbons with different freezing and boiling points. Magnetic properties of the colloid samples are measured by a vibrating sample magnetometer within a magnetic field range of ±1T. From the magnetization curves the specific magnetization of SNHMF, the particle magnetic moments distribution and the mean "magnetic" particle sizes of the samples are deduced. The particle hydrodynamic sizes (the solid magnetic phase with a surfactant layer) of the samples were verified by dynamic light scattering (DLS). The colligative properties, such as the vapor pressure, the freezing point and the osmotic pressure of SNHMF, are experimentally measured.

Key words: *hydrocarbon based magnetic fluid, surfactant-coated magnetic nanoparticles, colligative properties, magnetic properties*

---

1. INTRODUCTION

The use of high technology materials, such as magnetic fluids, in engineering applications has increased in recent years [1-5]. New engineering applications of magnetic fluids make it necessary to investigate their physical properties, including colligative ones. The physical properties of dilute solutions which depend only on the particle concentration of the solute, but not on the chemical composition, are called colligative properties. Colligative properties are also typical of colloidal solutions only in comparison with molecular solutions, they are less pronounced. This is due to the large mass of colloidal particles; the numerical density of the colloidal system is always much less than that of the molecular solution with the same mass concentration. As a rule, for true (molecular) solutions, with increasing concentration of the non-volatile component, main colligative properties appear, i.e. the vapor pressure above the solution decreases, the temperature of the freezing point and the osmotic pressure increase. The colligative properties of the colloids can play a very important role in the mass trans-capillary dynamics.

This study is aimed at determining the colligative properties of SNHMF and at qualitative comparison of these properties with those of classical molecular solutions and colloids with the isotropic interaction, as well as at investigating the influence of the external magnetic field on these properties.

SNHMFs are dispersions of magnetic single-domain nano-sized polydisperse in size and shape particles suspended in a carrier fluid. The colloidal stability and strong interaction between the particles and the dispersion medium are achieved by coating the particles with surfactant molecules. As the magnetic fluid (SNHMF) particle size (a magnetic nanoparticle with a chemically bounded surface-active layer), only 100 times exceeds the size of the carrier fluid molecules, at low concentration this system can be considered a pseudo-homogeneous environment with the isotropic interaction. The molecular kinetic equations which are appropriate for true (molecular) solutions are applicable to colloidal solutions with

a difference that the molar mass of the substance dissolved there is replaced by the colloidal particle mass [6]. If there is no excess of the surfactant in the system, at low concentrations, SNHMFs can be regarded as solutions which contain one non-volatile component (a magnetic nanoparticle with a chemically bounded surface-active layer). We start our investigations in these assumptions.

2. EXPERIMENTAL SECTION

2.1. Preparation of magnetic fluid samples

Some SNHMF samples were prepared on the base of dispersing fluids with different freezing and boiling points. The examined SNHMF consists of magnetite nanoparticles coated with oleic acid and suspended in different hydrocarbons. The studied SNHMF sample was prepared by the coprecipitation method according to the technology described in detail in [7-8]. Special treatment has been carried out to remove from colloid the excess of surfactant (i.e. the part not chemically bounded with nanoparticles). The density of the fluid was measured by the hydrometer for mineral oils.

2.2. Measurement of magnetic properties

The magnetic properties of the colloid samples were measured by a vibrating sample magnetometer (Lake Shore Co., model 7404 VSM) within a magnetic field range of ±1T [9-10]. As a result, typical magnetization curves of the samples were plotted (Fig. 1) and mathematically processed. The samples exhibit superparamagnetism because they show no hysteresis in their magnetization curves. The aim of the processing was to decompose the obtained curves into a sum of Langevin functions, each of which represents the dependence of the magnetization of a separate fraction of the superparamagnetic particles of the sample on the applied magnetic field, where n_i is the concentration number of the particles with the magnetic moment m_i.

$$M(H) = \sum_{i}^{N} n_i m_i L(m_i H/kT) \quad (1)$$

The Langevin function $L(x) = cth(x)-1/x$ describes the magnetization of one superparamagnetic particle. The set of n_i (i = 1, …, N) stands for the discrete distribution function for the particles with the magnetic moment m_i – it is a model parameter. If expression (1) is taken as the equation for n_i from the $M(H)$ data and from the predicted set m_i, this is an example of inverse task. The problem was solved numerically by solving the integral equation using the regularization method. From the obtained distribution, such parameters of the samples as the superparamagnetic saturation:

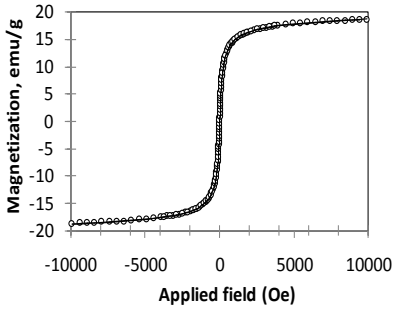

Fig. 1 MF-2 sample typical magnetization curve.

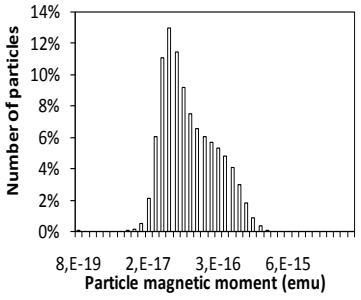

Fig. 2 Typical spectrum of particle magnetic moments of the MF-2 sample.

$$M_s = \sum_{i}^{N} n_i m_i , \quad (2)$$

the concentration of superparamagnetic particles:

$$n = \sum_{i}^{N} n_i , \quad (3)$$

and the mean magnetic moment of the particle:

$$\langle m \rangle = \sum_{i}^{N} n_i m_i / \sum_{i}^{N} n_i \quad (4)$$

are determined.

Under the assumption of spherical particles, the distribution of the magnetic moment may be transformed to the distribution of the particle size if assume $m_i = I_s \cdot \pi \cdot d_i^3/6$, where I_s is the estimated spontaneous magnetization of the particle material, d_i is the particle diameter. Accordingly, it is possible to estimate the mean particle diameter as

$$\langle d \rangle = (6 \cdot \langle m \rangle / I_s \cdot \pi)^{1/3} . \quad (5)$$

From the magnetization curves (Fig. 1, 2), the SNHMF specific magnetization, the spectrum of particle magnetic moments and the mean "magnetic" particle sizes of the samples are determined. The SNHMF characteristics are summarized in Table 1. The particle hydrodynamic sizes (the solid magnetic phase with a surfactant layer) of the samples

were verified by dynamic light scattering (DLS) (Zetasizer nano S90Malvern Instruments) which showed that the oleic acid surface layer thickness was ≈ 2 nm.

2.3. Freezing point determination.

The SNHMF freezing point was investigated using an experimental setup (Fig. 3), which consists of a cylindrical thermostated cell made of stainless steel. Hydrocarbon with the melting point ~282 K (pentadecane 99% $C_{15}H_{32}$ Aldrich) was used as a matrix, and oleic acid 99% $C_{18}H_{34}O_2$ Fluka was used as a surfactant to prevent particle agglomeration. The freezing points were measured by the temperature curve method because of its accuracy and simplicity [11]. The samples were frozen at relatively slow rates of temperature variation. The temperature in the cell can be set within 223–473 K and measured by a special bifilar wound copper thermal resistance probe up to an accuracy of 0.1 K. Electrical resistance was measured automatically every two seconds. The freezing point is derived from the relatively long temperature plateau of the time vs. temperature plot in Fig. 3. To study the magnetic field influence on the SNHMF freezing temperature, the cell was placed in an electromagnet which field intensity was controlled up to 0.65 T.

2.4. Measurement of vapor pressure.

The experimental setup for measuring the difference between the vapor pressure of the SNHMF and carrier fluid is shown in Fig. 4. The sealed cells with the magnetic fluid and carrier liquid are placed in a thermostat whose temperature can be varied from 273 to 423 K. The difference in vapor pressure between the magnetic fluid and the corresponding carrier medium with a known vapor pressure was measured at different temperatures. The pressure difference was measured by a U-shaped glass a manometer filled with di(2-ethylhexyl)sebacate (DOS).

Table -1 Samples under testing

Sample	**Carrier**	**Particles**	**Magnetization at 10 kOe, emu/cm^3**	**Most expected particle magnetic moment, emu**	**Concentration of particles 1/cm^3**	**Dipolar coupling parameter**
MF-1	Hexadecane $C_{16}H_{34}$	Magnetite Fe_3O_4 +oleic acid	15.8	2.27E-16	6.96E16	0.474
MF-2	Pentadecane $C_{15}H_{32}$	Magnetite Fe_3O_4 +oleic acid	10.2	3.1E-16	2.65E16	0.94
MF-3	Tetradecane $C_{14}H_{30}$	Magnetite Fe_3O_4 +oleic acid	18.4	6.24E-16	2.95E16	0.529
MF-4	Undecane $C_{11}H_{24}$	Magnetite Fe_3O_4 +oleic acid	12.5	1.25E-15	1.0E16	4.17
MF-5	Toluene C_7H_8	Magnetite Fe_3O_4 +oleic acid	11.9	2.5E-16	4.76E16	0.573
MF-6	Toluene C_7H_8	Magnetite Fe_3O_4 +oleic acid	5.95	1.3E-16	2.38E16	0.573
MF-7	Tetradecane $C_{14}H_{30}$	Magnetite Fe_3O_4 +oleic acid	12.5	1.7E-16	8.64E16	0.348
MF-8	Pentadecane $C_{15}H_{32}$	Magnetite Fe_3O_4 +oleic acid	3.2	3.52E-16	0.9E16	0.889
MF-9	Tetradecane $C_{14}H_{30}$	Magnetite Fe_3O_4 +oleic acid	4.4	1.4E-16	3.14E16	0.392

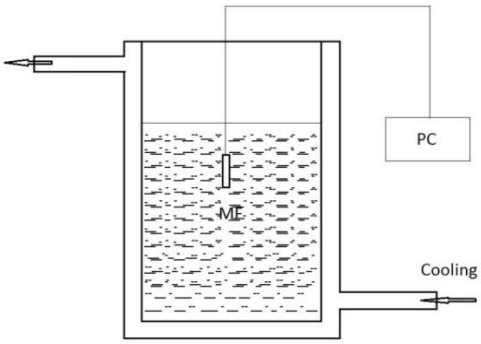

Fig. 3 The setup for measuring the magnetic fluid freezing point.

DOS has a low vapor pressure of $3.75 \cdot 10^{-3}$mm Hg at 473 K and the density 0.915 g/cm^3. The height difference of the DOS columns with a measurement accuracy of 0.01 mm was determined using a KM-8 cathetometer. Accordingly, in this experiment, the vapor pressure difference was measured at different temperatures. The effect of the possible magnetic field on the saturated pressure of SNHMF was tested as follows. A small permanent magnet was placed in the fluid in the thermostat. The magnetic fluid cell was exposed to the uniform field of this magnet with an intensity of 80 mT, and the pressure difference between the two cells was measured by the cathetometer KM-8 after the equilibrium state was achieved at the given temperature.

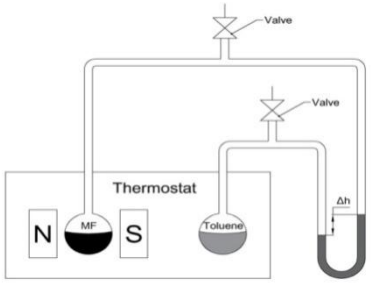

Fig. 4. The setup for measuring the vapor pressure.

2.5.Determination of osmotic pressure.

To determine the SNHMF osmotic pressure, a statistic method was applied. Two brass reservoirs (Fig. 5), containing, respectively, the magnetic fluid and the carrier liquid, are separated by a semi-permeable membrane made of cellophane. As the densities of the SNHMF and the carrier liquid are different, the pressure in each volume is measured separately. The levels of fluids are measured from the center of the membrane by the cathetometer KM-8 after the equilibrium state is achieved. Then the pressure difference is determined as

$$\Delta p = \rho_m g h - \rho_c g h, \quad (6)$$

where ρ_m, ρ_c are the densities of the magnetic fluid and carrier fluid, respectively.

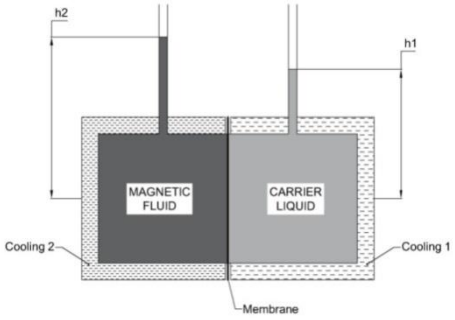

Fig. 5 The setup for measuring the osmotic pressure.

3. RESULTS AND DISCUSSION

3.1. Freezing point depression

Fig. 6A shows a PC processed curve of the freezing curve vs. time dependence of the sample MF-2. The curve is typical for a system with a non-volatile solute and a volatile solvent. A long freezing temperature plateau is observed. The freezing point is derived from this relatively long temperature plateau in Fig. 6B. At the freezing point of the substance, the solid and liquid phases are in equilibrium. The vapor pressures of the solid and liquid phases are the same at the freezing point. Diluting the $C_{15}H_{32}$ solvent by a non-volatile solute (magnetic particles with a surface layer) reduces the mole fraction of the $C_{15}H_{32}$ molecules and thus reduces the tendency of these molecules to escape not only into the vapor phase, but also into the solid phase. From the magnetic measurements, an average concentration of magnetic nanoparticles of $3.3 \cdot 10^{16}$ cm^{-3} $=1.51 \cdot 10^{-5}$ mol^{-1} was obtained. It seems that a solution with such a small concentration of magnetic particles can be considered ideal and describes a simple linear Raoult's relation between the freezing point depression and the molality of the solute [12]:

$$T\,(C_{15}H_{32}) - T\,(\text{SNHMF}) = \Delta\, T_f = \kappa_f\, m_c, \quad (7)$$

where $T\,(C_{15}H_{32})$ is freezing point of pentadecane, $T\,(\text{SNHMF})$ is freezing point of SNHMF, k_f is the cryoscopy constant of the solvent, and m_c is the colligative molality of the solution. The cryoscopy constant k_f of pentadecane was calculated by the formula

$$k_f = (R\, T_f^2)/ L_v, \quad (8)$$

where R is the molar gas constant, T_f is the freezing point and L_v is the enthalpy of the fusion of pentadecane and it was found to be k_f = 2.17 (K·kg)/mol.. From the measured concentration of magnetic nanoparticles, a very small decrease in freezing temperature can be theoretically deduced: $\Delta T_f = 4.8 \cdot 10^{-2}$ K. However, the experimentally obtained value ΔT_f = 3.4 K has a more significant meaning. A similar large decrease in freezing point ΔT_f was observed for the samples of other compositions: MF-1: 1.7 K, MF-4: 2 K. In SNHMF, the interaction between the nanoparticles and the carrier fluid is realized through the surfactant molecular non-polar free tails [13-14], whose numerical concentration is much larger than that of the magnetic nanoparticles. Apparently, this is the reason for the large difference between the theoretically predicted and experimentally measured freezing point of SNHMF.

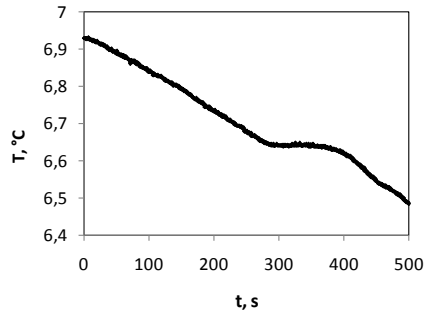

Fig. 6A Typical freezing curve of the sample MF-2.

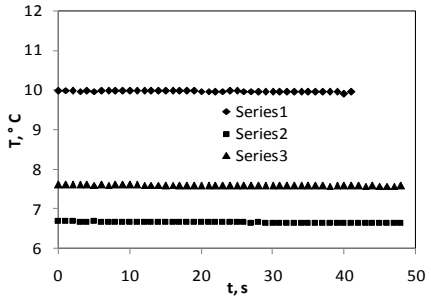

Fig. 6B The plateau of temperature vs. time curves: 1 – pentadecane, 2 – MF-2 in uniform magnetic field 0.62 T, 3 – MF-2.

At the freezing point temperature the vapor pressure of the solid equals the vapor pressure of the liquid and liquid and solid are in equilibrium. As a rule the vapor pressure decreases as the temperature decreases. The measured vapor pressure of solution is lower than that of solvent, so the vapor pressure of solution will equal that of the solid at lower temperature in the case of pure solvent. The equilibrium is achieved at a lower temperature at which the rate of freezing becomes equal to the rate of liquefying. Thus, the freezing point will be lower for a solution than for pure solvent.

Fig. 6B shows that the magnetic field initiates changes of the solid-liquid phase transition in the magnetic fluid. The presence of a uniform magnetic field increases the SNHMF freezing point. In an external magnetic field, the magnetic moments of the nanoparticles are oriented more or less parallel to the field, depending on the strength of the field, which leads to a decrease in entropy. Therefore, in order to liquefy the system in a magnetic field, it is necessary to increase the temperature.

3.2.Vapor pressure decrease

The dependence of the saturated vapor pressure on the temperature for toluene and sample MF-5 is presented in Fig. 7. Curve 1 is plotted from the data of reference [15] for toluene, and curve 2 is plotted from the experimental measurements of the difference in saturated vapor pressure between toluene and the MF-5 sample at different temperatures. At any given temperature, the vapor pressure of the magnetic fluid is less than that of pure toluene. Moreover, there is a significant difference between the experimentally measured saturated vapor pressure dependence on the molar concentration of the non-volatile substance (a magnetic nanoparticle with a surface layer) and the linear relationship of Raoult's law:

$$P_s = C_m P, \quad (9)$$

where P_s is the vapor pressure of the solution, C_m is the mole fraction of the solvent, and P is the vapor pressure of the pure solvent. From the magnetic measurements, the average concentration of magnetic nanoparticles $3.3 \cdot 10^{16}$ cm^{-3} = $2.38 \cdot 10^{-4}$ mol^{-1} for the MF-5 sample was obtained. Such small concentration of the non-volatile solute should create a negligible decrease in saturated vapor pressure compared to that for a pure solvent (toluene) at the same temperature. However, the experiment showed a significant reduction in vapor pressure for the magnetic fluid compared to the carrier medium (toluene) at all given temperatures. The boiling point of the magnetic fluid DF-5 increased approximately by 5 K if compared with toluene. As stated in section 3.1, the interaction of the nanoparticles and solvent molecules is realized through the surfactant (oleic acid) non-polar free tails, the numerical concentration of which is much larger than that of the magnetic nanoparticles. Apparently, this is the reason of such a large difference in saturated vapor pressure between the SNHMF and toluene. At a constant temperature in the uniform magnetic field 80 mT no dependence of the saturated vapor pressure on the field was observed. In the magnetic field, an ordered orientation of the magnetic moments of non-volatile nanoparticles occurred, which did not affect the properties of the carrier medium and, hence, the pressure of saturated vapors at a given temperature.

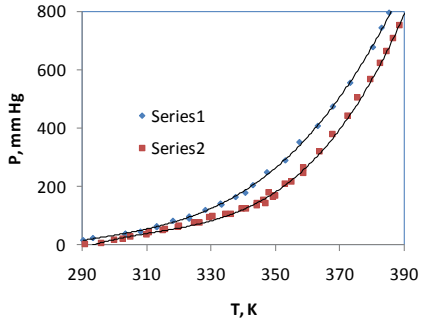

Fig. 7 Vapor pressure vs. temperature: 1 – toluene, 2 - MF-5.

3.3. Magnetic fluid osmotic pressure

Fig. 8 shows the osmotic pressure Π as a function of the number density n for different SNHMFs and their respective carrier media at a constant temperature of 293 K. The solid line conforms the Van't Hoff's ideal osmotic pressure formula:

$$\Pi = nkT, \quad (10)$$

where k is the Boltzmann constant. The values of triangles are measure experimentally for different SNHMFs by the osmometer (Fig. 5).

The osmotic pressure as a function of the concentration has been studied for colloids with the isotropic interaction [16-19] as well as with theoretical anisotropic [20-27] magnetic interactions for mono-disperse colloidal particles. Philipse and Kuipers reported a formula for the second virial coefficient B_2 of a dipolar hard-sphere fluid for a wide range of dipole moments in zero external field. For weakly interacting dipoles:

$$B_2/B_2^{HS}=1-(1/3)\lambda^2-(1/75)\lambda^4-(29/55126)\lambda^6, \quad (11)$$

here $B_2^{HS}=(2/3) - \pi d^3$ is the second virial coefficient of hard spheres with the diameter d, and $\lambda = \mu^2/kTd^3$ is the dipolar interaction coupling parameter, $\mu = (\pi d^3 m_s)/6$ is the magnitude of the dipole moment [27]. The second virial coefficient B_2 appears in the virial expansion of the osmotic pressure Π of a colloid with the number density n [17]:

$$\Pi/nkT=1 + B_2. \quad (12)$$

Formula (12) shows that, starting with non-magnetic hard spheres, the second virial coefficient monotonically decreases with increasing dipolar coupling parameter. As the dipolar mean forces are attractive, it gradually decreases the osmotic pressure of the fluid.

Experimentally, the osmotic equation of state has been derived for well-defined mono-disperse magnetic colloidal spheres that interact via a dipolar hard-sphere potential [29-30].The osmotic pressure was experimentally studied as a function of the colloidal number concentration, using a low-velocity analytical centrifuge and employing oleic acid coated monodisperse magnetite nanoparticles with the average diameter 13.4 nm (17.4 nm with the thickness of the oleic acid layer) in an organic solvent. The experimental osmotic pressure data initially follow Van't Hoffs law, but fall below it at n higher than$\approx 1.5\text{x}10^{-16}$ cm^{-3} (critical point). The dipolar coupling constant in the range λ = 2.0-2.4 was evaluated from the centrifugation experiments and at $\lambda \approx 1.8$ determined from the magnetization curves.

We investigated conventional SNHMFs containing single-domain polydisperse in size and shape magnetite particles. Qualitatively, the run of our experimental curve (Fig. 8, triangles) is consistent with that obtained in [29].

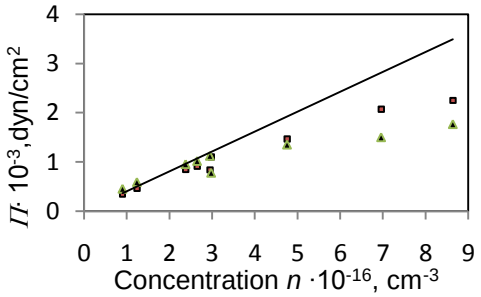

Fig. 8 Osmotic pressure dependence for different SNHMFs on their respective carrier media at 293 K: calculated data by Van´t Hoff´s law (solid line), calculated data by magnetization measurements (squares), experimental data (triangles).

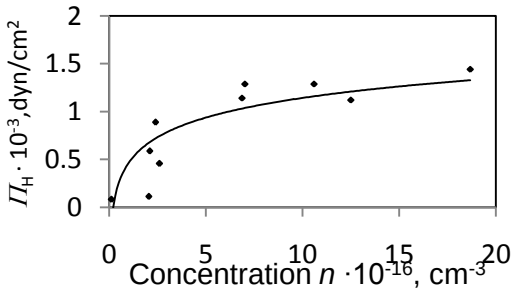

Fig. 9 Magneto-osmotic pressure dependence on the mean concentration of magnetic particles for different SNHMF samples at 293 K and magnetic field strength 1000 Oe.

Up to the magnetic nanoparticle concentration $n \approx 2.1\text{x}10^{16}\text{cm}^{-3}$, the experimental osmotic pressures nearly agree with Van't Hoff's law (10). At higher concentrations, the osmotic pressures fall below the values of Van´t Hoff´s law. This indicates that the bipolar attraction of the particles becomes stronger than the predicted hard sphere repulsion of the Carnahan-Starling equation.

To test the applicability of formulas (12), (13) for the estimation of the osmotic pressures of polydisperse magnetic fluids, the λ and B_2 values for different samples were determined from the magnetic measurements. The calculated osmotic pressure vs. particle concentration curve type (Fig. 8, squares) is similar to the experimentally obtained. Up to the magnetic nanoparticle concentration $n \approx 3 \cdot 10^{16}$ cm^{-3}, the calculated osmotic pressures nearly agree with Van´t Hoff´s law. However, the difference from Van´t Hoff´s law manifests itself later than for the experimentally obtained curve, and further all the Π values at the corresponding SNHMF concentration are larger than the experimentally obtained ones. The sample MF-4 is characterized by a relatively high magnetic coupling parameter λ = 4.17. If the second viral coefficient B_2 is calculated according to formula (12), the calculated osmotic pressure value drops sharply to the values of the other samples. Therefore, in this case the B_2 value was calculated according to the formula [22]:

$$B_2/B_2^{HS} \sim -exp(2\lambda)/12\,\lambda^2, \quad \lambda \rightarrow \infty. \qquad (13)$$

Adding the thus obtained B_2 value to formula (13) yields Π = 464 dyn/cm^2 at $n = 1.24\text{x}10^{16}$ cm^{-3}, which fits well the general trend $\Pi = \Pi(n)$. All these results indicate that it is possible to qualitatively assess the colligative properties of polydisperse SNHMFs from the dipolar coupling parameter λ obtained from the magnetization measurements.

Experimental determination of the osmotic pressure between the magnetic fluid and the carrier medium in the presence of an external magnetic field is quite a challenge. In any case, this is not possible with a semi-permeable membrane due to the occurrence of several adverse effects. Magnetic stresses at the interface produce a magnetic pressure [30] that affects the osmotic pressure measurements. At the same time, the effect is determined by the orientation of the field, e.g., the field directed perpendicular to the interface creates a higher pressure than its parallel orientation. In addition, the gradient magnetic field that arises at the contact surface (interface) between the magnetic fluid and the carrier fluid causes a particle magnetophoresis in the direction of the membrane.

Previously, the general case of structural transformations in the SNHMF exposed to an external magnetic field, considering the particle-particle interaction, has been analytically developed by Cebers in [31-32]. The work was done in the approximation of average mean effective field. In the framework of the mean effective field model, equations of state for the osmotic pressure have been derived:

$$\Pi = \frac{kTn}{1-nV} - \frac{1}{2}\gamma(nm)^2L^2(\xi), \qquad (14)$$

where $V = 4v$, v is the volume of a particle and γ takes the value 4π/3. The actual influence of the magnetic field on the osmotic pressure of the system is characterized by the second term in the right-hand side of equation (14). Using the average magnetic moment<m> and concentration<n> values of the particles obtained from the magnetic measurements, the second part of formula (14) was used to calculate the magneto-osmotic pressure values for a series of realistic magnetic fluids in the 1000 Oe field (Fig. 9). By comparing Figs. 8 and 9, one can see that the values of classical and magneto-osmotic pressures for magnetic fluids are approximately of equal order of magnitude.

4. CONCLUSIONS

In this paper, the colligative properties surfactant-coated nanoparticle hydrocarbon-based magnetic fluids were experimentally investigated. Different samples were prepared on the base of hydrocarbons as dispersing fluids, with different freezing and boiling points. Magnetic properties of the colloid samples were measured by a vibrating sample magnetometer in a magnetic field range of ±1T. It has been shown that the most expected parameter values obtained from magnetic measurements can be used to characterize the colligative properties of polydisperse SNHMFs. It is shown that if there is no free surfactant in the magnetic fluid, the systems can be considered as a pseudo-homogeneous environment and the magnetic fluid can be regarded as a solution which contains one non-volatile component (a magnetic nanoparticle with a chemically bounded surface-active layer). However, the experiment showed that the colligative properties of SNHMF, even at low concentrations, depend on both the surfactant and the dipolar coupling parameter. The effect of the uniform magnetic field on the colligative properties of magnetic fluids was investigated. It is found that the presence of a magnetic field increases the freezing temperature of the magnetic fluid but does not affect its boiling point. The magnetic field effect on the osmotic pressure was evaluated analytically. The magnetic field produces a noticeable effect on the osmotic pressure of magnetic fluids. It has been shown that it is possible to qualitatively assess the colligative properties of polydisperse SNHMFs from the dipolar coupling parameter λ obtained from magnetization measurements.

Acknowlegments

This work was financial supported by Latvian project: Nano, Quantum Technologies, and innovative materials for economics.

REFERENCES

[1]. Yooho Kim, G.A. Parada, S. Liu, X. Zhao, Ferromagnetic soft continuum robots, Sci. Robot. 4, 7329, 2019.
[2]. X. Zhao &Y. Kim, Soft microrobots controlled by nanomagnets, Nature v. 575, p. 58, 2019.
[3]. H. Yamaguchi and Y. Iwamoto, Heat transport with temperature-sensitive magnetic fluid for application to micro-cooling device, Magnetohydrodynamics, vol. 49, No. 3/4, 448-453, 2013.
[4]. V. Sreedharan, M.R. Anantharaman, Design and Fabrication of Micro-Transformer based on Ferrofluids, International Conference on Magnetic Fluids, July 8-12, 2019 Paris, Book of Abstracts, p.262.
[5]. H. Nishida, K. Shimada, Y. Ido, S. Fujioka, H.Yamamoto, Polishing characteristics by simultaneous imposition of magnetic and electrical fields utilizing a magnetic compound fluid, International Conference on Magnetic Fluids, July 8-12, 2019 Paris, Book of Abstracts, p.167.
[6]. Jean Babtiste Perrin, Traité de chimie physique. Les principles (1903) /Physical Chemistry Principles.
[7]. G.Kronkalns, Formation and magnetic properties of Mn-Zn ferrites nanoparticles, Magnetohydrodynamics, vol. 39, no. 2, (2003), pp. 215-223.
[8]. G. Kronkalns, A. Dreimane and M. M. Maiorov, The effect of thermal treatment on the magnetic properties of spinel ferrite nanoparticles in magnetic fluids, Magnetohydrodynamics, vol. 44, no. 1, 3-10, 2008.
[9]. A.Grants, A.Irbitis, G.Kronkalns, M.M.Maiorov. Rheological properties of magnetite magnetic fluid, J. Magn.Magn. Mat., vol. 85 (1990), 129-132.
[10]. M.M. Maiorov, E. Blums, K. Raj. Inverse task for evaluation of particle size distribution of polydisperse magnetic fluids. Proc. the12th International Conference on Magnetic Fluids. Physics Procedia 9 (2010) 74–77.
[11]. M.S. Rahman, N. Guizani, M. Al-Khaseibi, S. Al-Hinai, S.S. Al-Maskri, K. Al Hamhami, Analysis of cooling curve to determine the end point of freezing, Food Hydrocolloids 16 (2002) 653–659.
[12]. Kugel Roger, W.Raoult's low: Binary liquid-vapor phase diagram. J. Chemical Education, vol.75. 8, 1125.
[13]. Ayao Kitahara and Tatsuo Ishikawa, A study of the interaction between surfactants and hydrocarbon liquids by measurement of vapor pressure, J. Colloid and interface sci. 24, 189-192, (1967).
[14]. V. Ledovskykh, N. Stepanov, E. Freimantal, Influence of surfactants on surface tension and saturated vapor pressure of hydrocarbons, Proceedings of National Aviation University, Ukraine, no. 3(60), 2014, 98-102.
[15]. N.B. Vargaftik, Handbook of Thermophysical Properties of Gases and Liquids, Moscow, 1972, p. 720 (in Russ.).
[16]. N.F.Carnahan and K.E.Starling, Equation of state for non attracting spheres, J.Chem.Phys. vol. 51, No.2, p.635636 (1969).
[17]. Vrij A and Tuinier R 2005 Structure of concentrated colloidal dispersions, Fundamentals of Colloids and Interface Science,vol. 4, ed. J. Lyklema (Amsterdam: Elsevier).
[18]. H. Hansen-Goos and R. Roth, A new generalization of Carnaha-Starling equation of state to additive mixtures of hard spheres, J. Chem. Phys, v.124, 154506 (2006).
[19]. P.W. Rouw, A.T.J.M. Woutersen, B.J. Ackerson, C.G. De Kruif. Adhesive hard sphere dispersions: V. Observation of spinodal decomposition in a colloidal dispersionPhysica A: Statistical Mechanics and its Applications, Volume 156, Issue 3, Pages 876-898 (1989).
[20]. Piazza R, Bellini T and Degiorgio V, Equilibrium sedimentation profiles of screened charged colloids: A test of the hard-sphere equation of state, Phys. Rev. Lett.71, 4267, 1993.
[21]. Philipse A P and Vrij A. Determination of static and dynamic interactions between monodisperse, charged silica spheres in an optically matching, organic solvent, J. Phys. Chem. 88, 6459 (1988).
[22]. P. G. de GennesP. A. Pincus, Pair correlations in a ferromagnetic colloid, Phys. Kondens. Mater. v. 11, Issue 3, pp 189–198 (1970).
[23]. Chantrell R W, Bradbury A, Popplewell J and Charles, S W, Particle cluster configuration in magnetic fluids, J. Phys. D: Appl. Phys. 13 L119 (1980).
[24]. René van Roij,Theory of Chain Association versus Liquid Condensation, Phys. Rev. Lett. 76, 3348 (1996).
[25]. Teixeira P I C, Tavares J M and Telo da Gama M M, The effect of dipolar forces on the structure and thermodynamics of classical fluids 2000 J. Phys.: Condens. Matter 12 R411
[26]. Wang Z W, Holm C and Muller H W. Structure and rheology of ferrofluids: simulation results and kinetic models, Phys. Rev. E 66, 021405 (2002).
[27]. Philipse A P and Kuipers B M W 2010, Second virial coefficients of dipolar hard spheres, J. Phys.: Condens. Matter 22, 325104 (2010).
[28]. Bob Luigjes, Dominique M E Thies-Weesie, Albert P Philipse and Ben H Erne, Sedimentation equilibria of ferrofluids: I.Analytical centrifugation in ultra-thin glass capillaries, J. Phys.: Condens. Matter 24 (2012) 245103.
[29]. Bob Luigjes, Dominique M E Thies-Weesie, Ben H Ern´e and Albert P Philipse, Sedimentation equilibria of ferrofluids: II. Experimental osmotic equations of state of magnetite colloids, J. Phys.: Condens. Matter 24 (2012) 245104.
[30]. R. Rosensweig, Ferrohydrodynamics, Cambridge University Press, 1985, 344 p.

[31]. A.O. Cebers. Thermodynamic stability of magnetofluids, Magnetohydrodynamics, vol. 18, no. 2, 1982, 137-142.
[32]. E. Blums, A. Cebers and M.M. Maiorov, Magnetic Fluids, de Gruyter, Berlin, New York, 1997, 616 p.